

Spherical coded imagers: Improving lens speed, depth-of-field, and manufacturing yield through enhanced spherical aberration and compensating image processing

M. Dirk Robinson, Guotong Feng, and David G. Stork

Ricoh Innovations
2882 Sand Hill Rd, Suite 115
Menlo Park, CA 94025-7054

ABSTRACT

Recently, joint analysis and optimization of both the optical sub-system and the algorithmic capabilities of digital processing have created new digital-optical imaging systems with system-level benefits. We explore a special class of digital-optical imaging systems called *spherical coding* that combine lens systems having controlled amounts of spherical aberration with digital sharpening filters to achieve fast, low-cost, extended depth-of-field (EDoF) imaging systems. We provide analysis of the optimal amount of spherical aberration required as a function of desired depth-of-field extension. We also characterize the MSE-optimal filters required to restore contrast. Finally, we describe a simple method to designing spherical coded systems and demonstrate several advantages such as improved manufacturing yield using an actual lens design.

Keywords: digital imaging, optical design, image processing, EDoF, wavefront coding

1. INTRODUCTION

The majority of imaging systems rely on lenses with spherical surfaces because they are easy to manufacture and test even though they are sub-optimal for forming high quality optical images. Such departures from ideal imaging are broadly categorized into optical aberrations. During the last century, optical system design involved optimizing the shape, layout, and material properties of spherical lenses to minimize the optical aberrations inherent to spherical lenses in order to achieve the highest-contrast, sharpest optical image. Recently, joint analysis of both the optical sub-system and the algorithmic capabilities of digital processing have enabled new classes of *digital-optical* imaging systems.¹⁻³ This new joint digital-optical design approach can reduce system cost, improve manufacturing yield, and even transcend historic performance limitations. The key challenge in the digital-optical design framework is to balance efficiently the optical and digital components to maximize final image quality while satisfying design constraints.

In all of these digital-optical imaging systems, the final digital image depends on both the optical and the digital subsystems. In the simple case of image contrast information, the optical subsystem of a digital-optical system may not produce a blur-free optical image, but instead an optical image that may be sharpened via digital image sharpening. The digital sharpening restores lost contrast (removes image blur), at the expense of amplifying random imaging noise (reducing signal-to-noise (SNR)) inherent in the photodetection process. In this context, the goal of digital-optical design is one of balancing the contrast with image SNR by jointly optimizing both the optical and the image processing simultaneously.

We introduce a special digital-optical design concept called *spherical coding*, in which the optical designer deliberately allows or even enhances spherical aberration and then sharpens the blurry captured image using

Send correspondence to:
M. Dirk Robinson: E-mail: dirkr@rii.ricoh.com

digital post-processing thus achieving high-contrast imaging performance. Recent work applies spherical aberration to the design of microscope objectives for achieving only modest extension of the depth-of-field.⁴ This recent work shows certain extended depth-of-field advantages of spherical coding, but offers little insight into its broader benefits or tradeoffs. In this paper, we explore how the spherical coding framework provides other several system-level advantages: design simplicity, improved light collection (higher SNR) while extending the depth-of-field, and improved manufacturing yield.

Conceptually, spherical coding resembles wavefront coding techniques^{5,6} in which phase plates impart nontraditional aberrations whose image artifacts are then corrected by digital sharpening. Spherical coding, however, offers several advantages over such wavefront coding techniques. First, spherical coding requires only standard optical elements instead of unconventional rotationally-asymmetric elements⁵ or even exotic rotationally-symmetric aspheres.⁶ Using only standard optical elements simplifies both the manufacturing and testing of spherical coded systems and thus reducing the overall costs. Second, spherical coded systems comprised of spherical lens elements can be tested by traditional lens testing and alignment equipment. The rotationally-symmetric elements also do not require the rotational alignment of asymmetric wavefront coding elements. Third, the rotational symmetry of spherical aberration ensures polar symmetry of the effective digital-optical point-spread-function (PSF). In contrast, traditional cubic-phase wavefront coding lacks polar symmetry and has preferred axes of high quality at the expense of other axes.⁵

In Sect. 2, we review our framework for analyzing and designing digital-optical system from the end-to-end perspective. In Sec. 3 we introduce spherical coded imaging systems from the digital-optical perspective. In Sec. 3.1, we describe simple approaches to designing spherical coded systems and explore the advantages of spherical coding. In particular, in Sect. 3.2 we demonstrate the advantages of spherical coding for improved light-levels for extended depth-of-field imaging and describe the conditions under which spherical coding offers improved system-level performance. Section 3.3 details the improved tolerance of spherical coded systems to manufacturing errors. We conclude in Sect. 4 with a summary.

2. DIGITAL-OPTICAL SYSTEM ANALYSIS

Spherical coding is a special class of digital-optical imaging systems. In this section we introduce our analytical framework for designing and analyzing digital-optical imaging systems from an end-to-end perspective. The end-to-end perspective requires that we characterize the image system quality *after* digital processing. In this section, we review the concept of end-to-end image quality evaluation using image mean square error (MSE)¹ and show how to extend this to extended depth-of-field (EDoF) imaging applications.

2.1. End-to-end MSE image quality measure

The quality of an optical image depends on the wavefront error or optical-path-difference (OPD) function of the lens system. For rotationally-symmetrical optical systems, the wavefront error function is conveniently characterized using a set of polynomial functions known collectively as the Seidel aberrations.⁷ The Seidel aberration polynomial characterizes the wavefront error function $\Psi(\rho, \theta, h)$ at the exit pupil as a function of image field height h , and polar pupil coordinates ρ, θ . A third-order approximation of the wavefront error function using Seidel polynomials is given by

$$\Psi(\rho, \theta, h) = W_{02}\rho^2 + W_{04}\rho^4 + W_{131}h\rho^3 \sin(\theta) + W_{222}h^2\rho^2 \sin(2\theta) + W_{220}h^2\rho^2, \quad (1)$$

where W are the coefficients of the aberration polynomials (020-defocus, 040-spherical, 131-coma, 220-field curvature, 222 - astigmatism). These aberrations define the optical transfer function (OTF) according to the diffraction integral, which can be approximated as

$$H(\omega_1, \omega_2, h) = \mathcal{F}\{|\mathcal{F}\{A(\rho, \theta)e^{j2\pi\Psi(\rho, \theta, h)}\}|^2\}, \quad (2)$$

where $A(\rho, \theta)$ is the amplitude transmittance function of the exit pupil, \mathcal{F} the Fourier transform operator, and ω_i the spatial frequencies.⁸ In general, optical aberrations reduce image contrast by creating blurry

optical images. The magnitude of the OTF, $|H(\omega_1, \omega_2, h)|$, known as the modulation transfer function (MTF) characterizes the optical blur by quantifying the contrast preserved by the imaging system as a function of spatial frequency.

Most electro-optical imaging systems have sensors with sampling rates below the diffraction limit of the optical sub-system. The diffraction limit, which is approximately $\omega_D = 1/\lambda F\#$, is the highest spatial frequency resolved by the optical imaging system.⁸ The Nyquist rate of the digital-optical system depends on the pixel pitch P of the sensor and is given by $\omega_N = 1/2P$. We define the ratio between the Nyquist rate and the diffraction limit as the *undersampling factor* $U = \omega_N/\omega_D$. Typically, the quality of an optical imaging system is evaluated by examining the MTF value at the Nyquist rate ω_N . Optical design often involves optimizing the lens system to maximize the MTF at this sampling rate.

The traditional goal of the optical system designer is to minimize optical aberrations so as to ensure the optical image quality achieves a target contrast (MTF) at a specified spatial frequency, often the image sampling resolution ω_N . The optical system designer achieves this goal by shaping and arranging a sets of lens elements so that the aberrations imparted by individual lens elements balance each other and thus minimize geometric figures of merit such as the root-mean-square average of the wavefront error function (OPD-RMS) or the spot sizes (SS-RMS).⁹ Typically, increasing the performance requirements of an imaging system, such as the field-of-view, resolution, f-number, or spectral bandwidth, requires increasingly complex optical systems with more lens elements comprised of costlier materials. In this traditional design regime, a particular lens form, such as a triplet or doublet, has a prescribed performance range.⁷

In digital-optical system design, the optical image need not satisfy some image quality targets so long as the digital image, after processing, satisfies the desired performance target.¹ The digital image processing subsystem restores image contrast by applying sharpening filters tuned to the optical system's MTF. The ideal filter response for the OTF at a particular pixel location is the simple Wiener filter defined by

$$D(\omega_1, \omega_2) = \frac{T(\omega_1, \omega_2)H^*(\omega_1, \omega_2)}{|H(\omega_1, \omega_2)|^2 + \frac{\sigma^2}{S(\omega_1, \omega_2)}}, \quad (3)$$

where $S(\omega_1, \omega_2)$ represents the signal power spectral density (PSD) and σ^2 the noise power. The ratio of the average signal PSD over the noise power is the signal-to-noise ratio (SNR). A constant or flat signal PSD, such as $S(\omega_1, \omega_2) = 1000$ (or 30 dB SNR in log units), is commonly used. The term $T(\omega_1, \omega_2)$ represents the targeted MTF function. In this case, we use the aberration-free optical MTF as the targeted MTF function. In practice, the ideal Wiener filter response is difficult to implement fully so instead we approximate it using finite impulse response (FIR) filters.²

Figure 1 shows a simple example of the digital-optical imaging framework based on spherical coding. The optical MTF of a system blurred by two waves of spherical aberration shows lost contrast as lower MTF value, but never falls below a contrast value of 0.1 (dashed line in Fig. 1). The digital image processing system applies a Wiener filter whose spatial frequency response is shown as the dotted line. The effective system MTF (optical + digital systems) shows restored image contrast (solid line). The images in the right side of Fig. 1 shows an example of a captured image blurred by spherical aberration and the restored image after digital processing. The blurry captured image is visually similar to those images captured by *soft* lenses used in portraiture. After processing, however, the image shows the sharpness of a well-designed traditional optical system.

The means of combining a contrast-based optical figure of quality with an SNR-based digital figure of merit capturing the end-to-end image quality is by way of mean-square-error (MSE) or root-mean-square-error (RMSE). For a given optical transfer function, digital filter response, and signal PSD and noise power, the digital-optical MSE is given by

$$MSE(H, D) = \frac{1}{4\omega_N^2} \int_{-\omega_N}^{\omega_N} \int_{-\omega_N}^{\omega_N} S(\omega_1, \omega_2) |T(\omega_1, \omega_2) - H(\omega_1, \omega_2)D(\omega_1, \omega_2)|^2 + \sigma^2 |D(\omega_1, \omega_2)|^2 d\omega_1 d\omega_2 \quad (4)$$

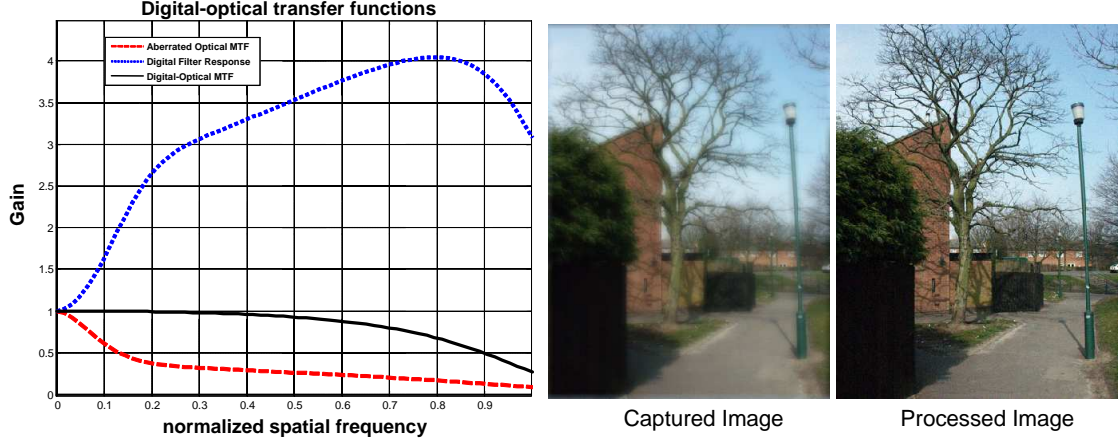


Figure 1. The curves on the left graph show the transfer functions for a spherically aberrated optical system (dashed), a compensating digital filter (dotted), and the combined digital-optical transfer function (solid). The center image shows a captured image degraded by spherical aberration. The image on the right shows the image after application of the digital compensation filter.

$$= \gamma + \sigma_P^2. \quad (5)$$

The term γ captures the average departure from the ideal MTF function weighted by the signal PSD. The term σ_P^2 captures the average noise power after application of the digital sharpening filter. In digital-optical design, both the optical system and the digital subsystem are optimized based on this end-to-end MSE performance criterion.¹ For many well-designed digital-optical imaging systems, the optical MTF does not fall below some critical threshold, such as 0.1. Consequently, a well-designed digital filter will restore the system MTF leading to the case where the MSE is dominated by the system noise power σ_P^2 . The *noise gain* of the digital system is given by $g = \sigma_P^2/\sigma^2$. For example, the noise gain for system of Fig. 1 corresponds to about $3\times$ the noise in the original captured images, or less than 2 bits of dynamic range. For many systems, such a noise gain is nearly imperceptible and is often less than bit loss incurred by common digital image compression algorithms.

2.2. EDoF digital-optical imaging systems

In the case of extended depth-of-field (EDoF) imaging systems, a single digital filter $D(\omega_1, \omega_2)$ must restore the MTF for a range of possible object distances. In this case, the MSE formula of Eq. 4 is extended to include integration over a range of defocus aberration polynomial coefficients $W_{02} \in [-r, r]$,

$$MSE(H, D, r) = \frac{1}{8r\omega_N^2} \int_{-r}^r \int_{-\omega_N}^{\omega_N} \int_{-\omega_N}^{\omega_N} S(\omega_1, \omega_2) |T(\omega_1, \omega_2) - H(\omega_1, \omega_2, W_{02})D(\omega_1, \omega_2)|^2 + \sigma^2 |D(\omega_1, \omega_2)|^2 d\omega_1 d\omega_2 dW_{02} \quad (6)$$

The ideal EDoF Wiener filter over the range of defocus has the spectral response

$$D(\omega_1, \omega_2, r) = \frac{S(\omega_1, \omega_2) \bar{H}^*(\omega_1, \omega_2, r)}{S(\omega_1, \omega_2) \bar{H}^2(\omega_1, \omega_2, r) + \sigma^2}, \quad (8)$$

where

$$\bar{H}(\omega_1, \omega_2, r) = \frac{1}{2R} \int_{-r}^r H(\omega_1, \omega_2, W_{02}) dW_{02} \quad (9)$$

$$\check{H}^2(\omega_1, \omega_2, r) = \frac{1}{2R} \int_{-r}^r |H(\omega_1, \omega_2, W_{02})|^2 dW_{02}. \quad (10)$$

We insert this EDoF Wiener filter into Eq. 7 to obtain the predicted EDoF MSE:

$$MSE(r) = \frac{1}{8r\omega_N^2} \int_{-\omega_N}^{\omega_N} \int_{-\omega_N}^{\omega_N} \frac{S(\omega_1, \omega_2)\sigma^2 + S^2(\omega_1, \omega_2) [\check{H}^2(\omega_1, \omega_2, r) - \bar{H}^2(\omega_1, \omega_2, r)]}{S(\omega_1, \omega_2)\check{H}^2(\omega_1, \omega_2, r) + \sigma^2}. \quad (11)$$

Equation 11 shows that the predicted MSE depends on two components. The first relates to the image quality using the average of the MTF over the depth volume. The second term is proportional to the variance of MTF over the depth range $[\check{H}^2(\omega_1, \omega_2, R) - \bar{H}^2(\omega_1, \omega_2, R)]$. In the case of wavefront coding, this second term is very small wavefront as the MTFs are nearly depth-invariant.

3. INTRODUCTION TO SPHERICAL CODING

Spherical coding is a special class of digital-optical design that relies primarily on spherical aberration to achieve system-level advantages. Spherical aberration has several advantages from the digital-optical system perspective. For example, of all the Siedel aberrations, only spherical aberration reduces contrast in a rotationally-symmetric, field-invariant fashion thus simplifying the design of the digital subsystem. Field-invariant aberrations require only a single, space-invariant sharpening filter to restore contrast over the entire image. Also, the polar-symmetry of the optical aberration, and hence MTF, demand rotationally-symmetric filters. This simple polar symmetry reduces the complexity of the digital filters. For example, polar symmetry allows simple symmetric FIR filters which are easy to design.¹ Finally, the science of optical engineering has collected a comprehensive understanding the most basic aberration, namely spherical aberration, and its relationship to lens system layout.⁹

In the remainder of this section, we explore a simple single BK7 lens spherical coded imaging system illustrating the key advantages of lowering optical complexity, extending the depth-of-field, and improving manufacturing yield. The nominal system is a $f = 10\text{mm}$ focal length, $F\#4.5$, 25 degree field-of-view (FOV) monochromatic imaging systems at the green wavelength of 550 nm. The design degrees of freedom include the front aperture stop location, the lens curvatures, and the back focal distance.

As a point of comparison, we compare our spherical coded singlet with two traditional optical system designs. Both layouts and optical MTFs are shown in Fig. 2. Both systems are optimal in the sense of having minimal OPD-RMS over the image field. The first design is a triplet system based on a triplet comprised of three BK7 spherical lens elements as shown in the left side of Fig. 2. The system is very well corrected showing nearly diffraction-limited MTF performance. The system has less than 0.5 waves of spherical aberration. The second design is a doublet BK7 lens. The design form limitation of the traditional doublet lens system increases the spherical aberration to about 1.05 waves. The doublet system shows reasonably good contrast over a wide range of spatial frequencies throughout the 24 degree FOV. Both systems represent significantly more complex optical systems than the singlet system in order to balance the optical aberrations of the imaging system operating at the relatively fast speed of $F\#4.5$.

3.1. Designing spherical coded systems

Many commercial lens design software tools, such as Zemax and OSLO, provide direct measurements of spherical aberration coefficients. This feature enables a simple approach to designing spherical coded systems. By adding a constraint on the spherical aberration coefficient to a traditional wavefront error (e.g. OPD-RMS) merit function, a system designer can minimize the spatially-varying optical aberrations such as coma, astigmatism, and field curvature at the expense of spherical aberration. While this approach requires some manual intervention to tune the strength of the spherical aberration, it does not require the complex digital-optical simulation and optimization software described in prior work.¹ In practice, using the full joint optimization tools, however, will produce higher quality digital-optical systems. The designer can roughly

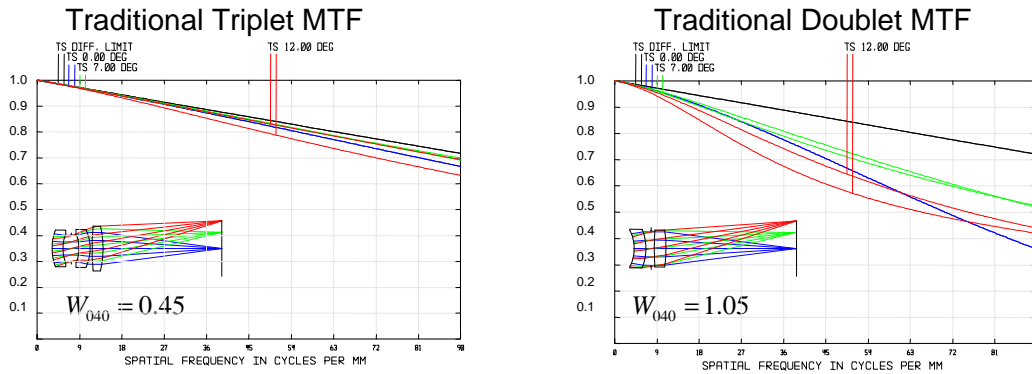


Figure 2. The left graphs show the layout and MTF of a well-corrected triplet imaging system having less than 0.5 waves of spherical aberration. The system shows nearly diffraction-limited MTF performance over a wide range of spatial frequencies. The graph on the right shows the layout and MTF of a reasonably well-corrected doublet imaging system. The doublet system has about 1.1 waves of spherical aberration and shows moderate contrast loss throughout the image field. Both systems, however, provide reasonable optical contrast and represent the traditional approach to optical imaging system design.

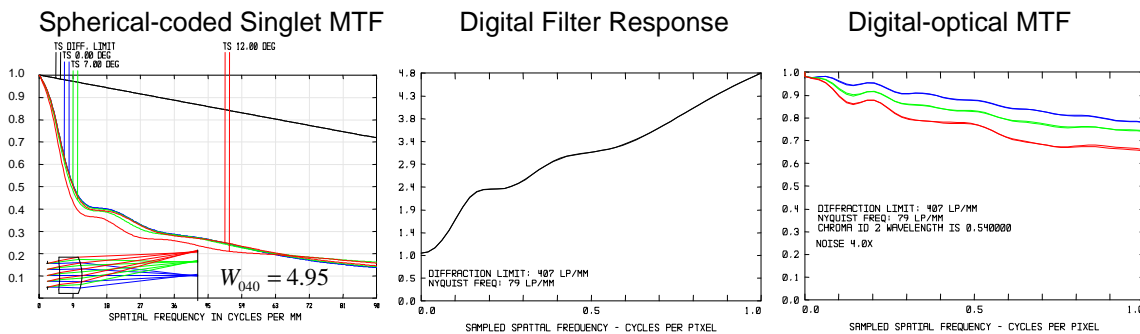


Figure 3. The left graphs show the MTF of a spherical coded singlet system optimized by minimizing OPD-RMS while maintaining 5 waves of spherical aberration at $F\#4.5$. The center curve shows the frequency response of the spatially-invariant filter used to restore the image contrast for a system with a sampling rate of 79 lp/mm ($6.3 \mu\text{m}$ pixel pitch). The curve on the right shows the effective system MTF *after* application of the digital filter. After filtering, the digital-optical system shows acceptable contrast throughout the sampled spatial frequency range with only a moderate noise gain of $4\times$.

evaluate the quality of the digital-optical design by direct examination of the MTF curves to verify that the values do not fall below the critical threshold of 0.1 throughout the sampling band and that the MTF curves overlap showing approximate spatial-invariance.

As an example, the left graph of Fig. 3 shows the MTF curves for a spherical coded singlet. The singlet was optimized by minimizing the OPD-RMS while constraining the spherical aberration to be $W_{04} = 5$ waves. The MTF curves show the characteristic drop off in MTF at low spatial frequencies but never falling below a threshold of 0.1 below which signal restoration becomes difficult. The MTF curves, however, are relatively uniform over the image field; thus simple spatially-invariant filters can restore contrast.

The center curve of Fig. 3 shows the frequency response of the spatially-invariant filter used to restore the image contrast for a system with a sampling rate of 79 lp/mm ($6.3 \mu\text{m}$ pixel pitch). The frequency

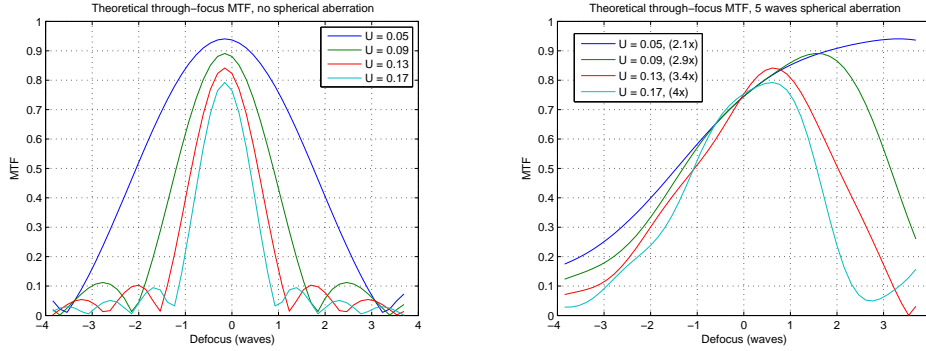


Figure 4. The left curves compare the theoretical through-focus MTF curves for an aberration-free optical system at several normalized spatial frequencies (U). The curves show the characteristic symmetric through-focus MTF shape. The right curves compare the theoretical through-focus MTF curves for a system having $W_{040} = 5$ waves of spherical aberration after application of sharpening filters optimized over the range $W_{02} \in [-1, 1]$ using Eq. 8 at several normalized spatial frequencies. This theoretical spherical-coded system shows broader shape indicating the extended depth-of-field.

response of this filter is approximately rotationally symmetric. The curve on the right shows the effective system MTF *after* application of the digital filter. After filtering, the digital-optical system shows acceptable contrast throughout the sampled spatial frequency range with only a moderate noise gain of $4\times$.

The triplet and doublet lens systems represent the traditional approach of using more expensive optical systems (multiple elements) to balance aberrations and achieve acceptable system contrast. The spherical coded singlet design demonstrates the ability of spherical coding to extend a simple lens forms beyond its conventional limits by using digital post-processing. In essence, this allows the design to tradeoff optical for digital subsystem cost to achieve system contrast. While the digital-optical system also pays a SNR penalty, in certain applications, this tradeoff may be acceptable. Also, as we shall see in the next sections, the spherical coding philosophy also improves depth-of-field and manufacturing yield.

3.2. Advantage 1: Extended depth-of-field

Some of the robustness properties of spherical coding can be explained by its ability to moderately extend the depth-of-focus (and hence depth-of-field) in a fashion similar to that of wavefront coding.⁵ The combination of spherical aberration and digital processing extends the depth-of-field (EDoF) eliminating the need for either stopping down the lens or mechanical actuation. Thus, the digital-optical approach to depth-of-field extension can provide considerable cost savings.

In the context of end-to-end performance, the depth-of-focus of the digital-optical system is defined by the range of focus $W_{02} \in [-R, R]$ for which a criterion contrast is preserved. For example, the left graph of Fig. 4 shows the through-focus MTF performance of an ideal aberration-free optical system for several spatial frequencies normalized by the diffraction-limited spatial frequency. The depth-of-focus is approximately the range of defocus within which the MTF preserves contrast above a threshold such as 0.3. For example, for a low-resolution system with maximum resolution corresponding to of $U = 0.05$, the depth-of-focus is about 5 waves of defocus. The higher resolution system $U = 0.17$ tolerates only about 1.5 waves of defocus.

The graph on the right side of Fig. 4 compares the through-focus system MTF (after sharpening) for a theoretical spherical-coded system having $W_{040} = 5$ waves of spherical aberration. The sharpening filters were optimized using Eq. 8 for a range of defocus $W_{02} \in [-1, 1]$. The effective SNR penalty ranges from about $2\times$ to $4\times$. The through-focus MTF curves after sharpening show considerably broader depth-of-focus than

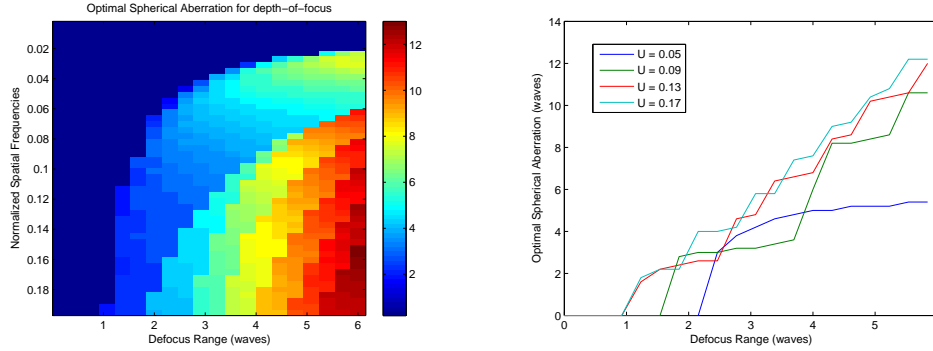


Figure 5. The image on the left shows the optimal amount of spherical aberration (W_{040}) in waves which minimizes RMSE over a range of defocus (W_{02}). The horizontal axis represents the range of defocus in waves and the vertical axis represents the undersampling factor (relative resolution) of system. The curves on the right show horizontal slices through the image on the left at a few undersampling factors. The optimal system has no spherical aberration up to a defocus range that depends on the undersampling factor. Above that value, the optimal amount of spherical aberration increases in step-like functions which depend on the defocus range.

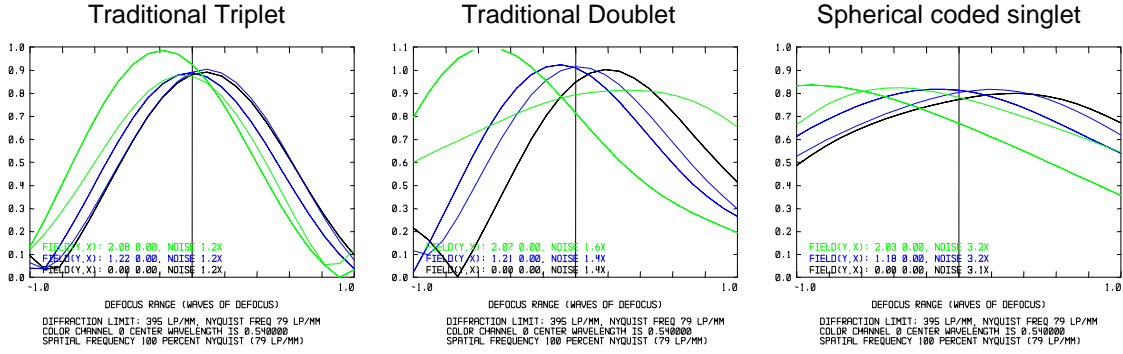
those of the diffraction-limited system of Fig. 4. For example, the high-resolution system $U = 0.17$ shows a depth-of-focus of about 3 waves, nearly twice that of the aberration-free system.

We observe that the optical focus locations, or peak MTF values, are not aligned for the different spatial frequencies as they are in the case of the diffraction-limited system. This implies that the optimal focus location for a spherical-coded system depends on the system undersampling factor U . In many cases, the MSE-optimal focus for a spherical coded system with positive spherical aberration is behind both the paraxial and OPD-RMS minimizing back focal distance.

Since introducing spherical aberration into the optical system incurs an SNR penalty, it is important to identify the ideal amount of spherical aberration for a desired depth-of-focus range. We perform an exhaustive search to find the optimal amount of spherical aberration for a given defocus range $2R$ and undersampling factor U . We assume a flat signal PSD function with SNR of 30 dB. As we observe in the right side of Fig. 4, the through-focus MTF peak varies as a function of spatial frequency in a spherically-aberrated optical system suggesting that the optimal focal plane depends on the undersampling factor U . Consequently, for every undersampling factor, depth-range, and amount of spherical aberration we identify the MSE-optimal focal distance. Then, we identify the optimal amount of spherical aberration minimizing MSE over the desired focal depth range (in waves).

The left image of Fig. 5 shows the optimal amount of spherical aberration for different undersampling factors (vertical) and different depth ranges (horizontal). The right graph of Fig. 5 shows four different slices through this image. As we expect, when the depth range is small enough such that the aberration-free optical system provides sufficient contrast, the optimal amount of spherical aberration is zero (left side). For example, at undersampling factor $U = 0.17$, the MSE-optimal amount of spherical aberration for a defocus range of $2R = 2$ waves is about 4 waves of spherical aberration. The step-like increase in the optimal spherical aberration relates to the number of MTF zero-crossings inherent to the defocus aberration.

Real optical systems contain aberrations other than defocus and spherical aberration alone. Figure 6 compares the through-focus MTF curves *after* application of optimal EDoF Wiener filters for the three optical system described previously for several field angles. All three plots show the through-focus MTF for a system with maximum resolution corresponding to approximately $U = 0.2$. The left two curves show the through-focus for the traditional triplet and doublet systems. The traditional triplet shows the small focal range nearly identical to that of the theoretical aberration-free system of Fig. 4. The doublet system



Through-Focus Digital-optical MTF

Figure 6. The three graphs show the through-focus MTF curves at the sampling frequency 79 lp/mm after application of the MSE-optimal EDoF Wiener filter defined in Eq. 8. The three curves within each plot show the through-focus MTF curves for the 0, 70, and 100 % full-field angles. The curves for the triplet system (left) show traditional narrow depth-of-field through-focus MTF curves similar to an aberration-free system. The curves for the doublet system (center) show both the narrow depth-of-field of an aberration-free system on-axis, but also show the effects of astigmatism and field curvature for the off-axis field angles. These off-axis aberrations further reduce the depth-of-focus throughout the image field. The spherical coded singlet curves (right) show the extended depth-of-field capability with only moderate field-curvature and astigmatism.

show both narrow depth-of-field as well as poor field invariance. The off-axis field locations show considerable astigmatic through-focus curves due to the limitations of the doublet lens form. The through-focus curves on the right show the spherical coded singlet system. While the system shows small amounts of field-curvature and astigmatism, the through-focus curves are broad indicating the EDoF imaging capability throughout the field of view. While an opto-mechanical focus mechanism would enable the traditional system to re-focus on a depth plane of interest, adding such opto-mechanical system would incur considerable expense and electrical power when compared to a fixed-focus lens system.

3.3. Advantage 2: Improved Manufacturing Tolerance

Errors in optical imaging systems arise from a multitude of process variations from fabrication to assembly. Common process variations create surface power, wedge, decentration, and thickness errors as well as element tilt, decenter, and spacing errors.⁷ Many of the random process variations create either pupil-dependent or field-dependent focus errors which degrade optical MTF at various spatial frequencies. Intentionally adding spherical aberration to an optical system can make the MTF of the optical system less sensitive to many of the process variations due to the associated moderate depth-of-focus extension. The spherical aberration introduced by during the spherical coding design stage can mask many of the focus-related aberrations imparted due to manufacturing errors. In keeping with the digital-optical framework, we consider the digital filtering as a type of digital compensation for the optical manufacturing and assembly errors. Digital-only compensation is significantly cheaper than the traditional opto-mechanical compensation techniques such as back-focus adjustment.

In this section, we evaluate the yield of our three different imaging systems based on the final digital-optical RMSE image quality metric. We perform 300 Monte Carlo (MC) simulations using Gaussian random variables for the standard manufacturing tolerances shown in Table 3.3. We assume that each as-built optical system undergoes an MTF test that provides accurate measurement of MTF throughout the image field. This MTF information is used to design MSE-optimal Wiener filters for each optical system using Eq. 3. We

Parameter	Standard deviation
lens thickness	100 μm
surface radius	1 fringe
surface tilt	50 μm
surface decenter	50 μm
element tilt	.05 degrees
element decenter	50 μm

Table 1. The optical manufacturing tolerances expressed as the standard deviation of each random variable.

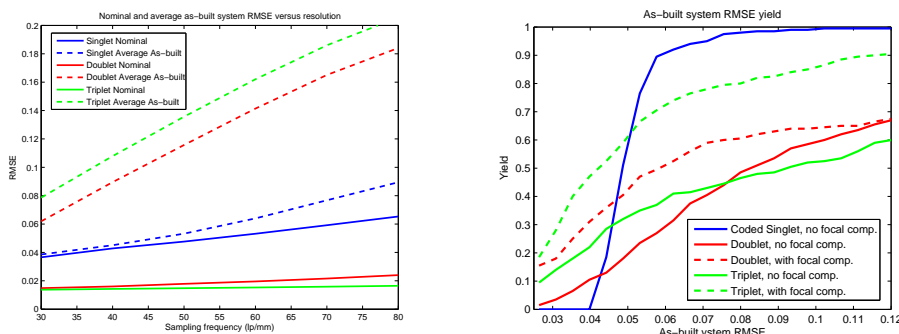


Figure 7. The left plot compares the nominal and average as-built RMSE performance of the spherical coded (blue), uncoded traditional doublet (red), and triplet (green) systems as a function of the sampling rate (pixel pitch). The uncoded systems show superior nominal RMSE performance over the nominal spherical coded design. The average RMSE performance of the spherical coded systems, however, are far superior to the average RMSE performance of the traditional designs. The right graph compares the RMSE cdf function of the three systems (solid) using only digital filter compensation for a sampling resolution of 50 lp/mm. The dashed curves show the improved gained by adding opto-mechanical back focus compensation to the traditional doublet and triplet systems. Even with expensive optical compensation, the spherical coded systems show superior yield for the reasonable RMSE image quality of 0.08.

assume a flat signal PSD and a system with SNR of 30 dB and then evaluated the final image quality using the RMSE metric of Eq. 4 for every as-built system over a range of possible image resolutions including 30, 40, 50, 60, 70, and 80 lp/mm.

The left graph of Fig. 7 compares the nominal RMSE (solid) for the three systems with the average RMSE (dashed) value over the collection of 300 random as-built systems. As expected, the nominal triplet and the doublet optical system show the very high quality RMSE performance (less than $RMSE < 0.02$) indicative of nearly diffraction-limited performance. The nominal spherical coded singlet provides image roughly twice the error of the triplet ($RMSE = 0.04$) due to the SNR loss inherent in the sharpening process. Yet, we observe that the average as-built RMSE for the spherical coded singlet is only slightly worse than the nominal system. The as-built performance of the traditional triplet and doublet systems are significantly worse. The solid curves in the right side of Fig. 7 show the cumulative distribution function (cdf) of the RMSE for the systems having a sampling rate of 50 lp/mm. For this system, an RMSE of 0.08 corresponds to roughly two bits of error due to noise loss. We find that this is the maximum allowable SNR loss that provides visually acceptable results. We observe that only a small percentage (50%) of traditional systems show RMSE performance less than 0.08. Nearly 95% of the as-built spherical coded systems show RMSE performance less than 0.08.

The dashed curves in the right side of Fig. 7 show that the RMSE performance improves when adding an expensive opto-mechanical back focus optical compensation to the traditional systems. The focal com-

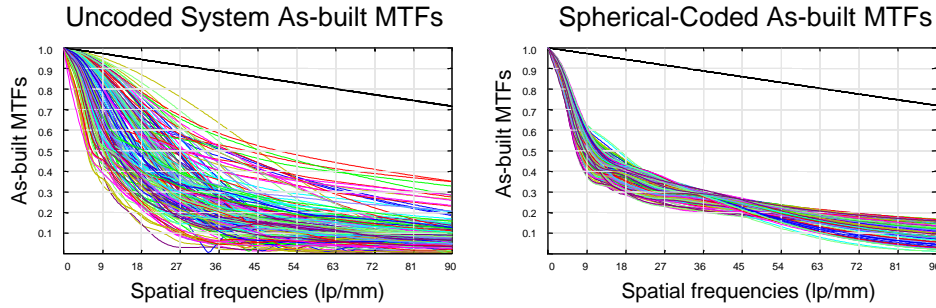


Figure 8. Both graphs show twenty as-built optical MTF curves for the uncoded doublet systems (left) and the spherical coded singlet (right). The solid black line shows the diffraction-limited MTF. The traditional doublet shows wild variation in MTF performance whereas the as-built MTF curves of the spherical coded singlet show much tighter range. The majority of these systems can be corrected with digital processing, thereby increasing yield.

pensation enables OPD-RMS optimal refocus prior to digital compensation, and RMSE evaluation. While the back focus compensation doubles the yield for high-performance systems ($RMSE < 0.04$), the yield at RMSE of 0.08 is still bested by the spherical coded systems. This demonstrates the ability of spherical coding to provide high-yield drop-in fixed-focus optical systems at a much lower cost than the traditional.

The improvement in performance is explained in part by the sacrificing of the MTF at low spatial frequencies to increase defocus tolerance at high spatial frequencies. Also, the singlet system has fewer degrees of freedom and hence reduces the chances of random manufacturing errors from accumulating to reduce image quality. We observe this if we compare the MTF curves for some of the as-built uncoded doublets shown in the left side of Fig. 8 with those of the coded singlet shown in the right side of Fig. 8. The uncoded singlet design shows many as-built systems whose optical MTF does not fall below 0.5 before 30 lp/mm whereas almost all of the the coded singlet systems have MTF of 0.5 at 10 lp/mm. The spherical coded singlet, however, preserves contrast out to nearly 70 lp/mm for most of the as-built systems. Thus, while the spherical coded systems have much poorer nominal MTF, the transfer function is such that digital sharpening can restore contrast without loss of information due to zero-crossings in the MTF. Furthermore, since the as-built MTF functions do not vary considerably, we could imagine using a static restoration filter for the as-built systems with reasonable results.

4. CONCLUSION

We introduced a special class of digital-optical systems called spherical coded systems that intentionally introduce spherical aberration into an optical system followed by digital sharpening to achieve system level benefits such as depth-of-field extension, low f-number, and improved manufacturing yield. We provide simple approaches to designing such systems and show the optimal amount of spherical aberration required to achieve a certain depth-of-field extension. Finally, we demonstrate the advantages of spherical coding for a simple imaging system. The concept of spherical coding is broadly applicable to a variety of imaging systems applications, by providing the system designer a simple method for trading off digital image SNR with optical performance characteristics such as lens complexity and yield.

REFERENCES

1. D. G. Stork and M. D. Robinson, "Theoretical foundations for joint digital-optical analysis of electro-optical imaging systems," *Applied Optics*, April 2008.

2. M. D. Robinson and D. G. Stork, "Joint design of lens system and digital image processing," in *Proceedings of the International Optical Design Conference*, G. Gregory, J. Howard, and J. Koshel, eds., **6342**, OSA, August 2006.
3. M. D. Robinson and D. G. Stork, "End-to-end compensation of digital-optical imaging systems," in *Proceedings of the SPIE*, W. J. S. Pantazis Z. Mouroulis and R. B. Johnson, eds., **6288**, SPIE, August 2006.
4. P. Mouroulis, "Depth of field extension with spherical optics," *Optics Express* **16**(17), pp. 12995–13004, 2008.
5. W. T. Cathey and E. Dowski, "A new paradigm for imaging systems," *Applied Optics* **41**(29), pp. 6080–6092, 2002.
6. W. Chi and N. George, "Electronic imaging using a logarithmic asphere," *Optics Letters* **26**(12), 2001.
7. W. J. Smith, *Modern Optical Engineering*, McGraw-Hill, New York, NY, 2000.
8. J. W. Goodman, *Introduction to Fourier Optics*, McGraw-Hill, New York, NY, second ed., 1986.
9. R. E. Fischer and B. Tadic-Galeb, *Optical System Design*, McGraw-Hill, New York, 2000.